Available online at www.sciencedirect.com
SCIENCE DIRECT®
Journal of Sound and Vibration 288 (2005) 847–863
JOURNAL OF SOUND AND VIBRATION
www.elsevier.com/locate/jsvi

Non-dimensional analysis and design of a magnetorheological damper

S.R. Hong[a], S.B. Choi[a,*], Y.T. Choi[b], N.M. Wereley[b]

[a]*Smart Structures and Systems Laboratory, Department of Mechanical Engineering, Inha University, Incheon 402-751, Korea*
[b]*Smart Structures Laboratory, Department of Aerospace Engineering, University of Maryland, College Park, MD 20742, USA*

Received 27 July 2004; received in revised form 4 January 2005; accepted 13 January 2005
Available online 31 May 2005

Abstract

This paper presents a non-dimensional design scheme for a magnetorheological (MR) mixed-mode damper. Based on the Bingham plastic constitutive equation of the MR fluid, four non-dimensional design parameters are defined: Bingham number, non-dimensional damping force, dynamic range and geometric ratio. After investigating the design characteristics of each parameter, sequential design steps for the MR damper are formulated. A single dof vibration model consisting of a spring and an MR damper is then utilized to demonstrate the effectiveness of the proposed design methodology. By imposing equality constraints on required damping force and dynamic range of the vibration model, the principal design parameters, such as electrode length, can be determined from the non-dimensional analysis. Subsequently, the MR damper is manufactured and its measured damping force characteristics are evaluated and compared with the predicted results.

1. Introduction

Electrorheological (ER) and magnetorheological (MR) fluids undergo reversible and rapid changes in material characteristics when subjected to electric and magnetic fields, respectively.

*Corresponding author. Tel.: +82 32 860 7319; fax: +82 32 868 1716.
E-mail address: seungbok@inha.ac.kr (S.B. Choi).

0022-460X/$ - see front matter © 2005 Elsevier Ltd. All rights reserved.
doi:10.1016/j.jsv.2005.01.049

Nomenclature

a, b, c	coefficients of the non-dimensional equation
A_p	piston head area
c_f	fluid damping constant
c_r	rubber damping constant
c_{sky}	gain of the sky-hook controller
f_c	control force
F_{mr}	maximum damping force
F_v	viscous damping force
h	gap size
H	magnetic field intensity
k_r	rubber spring constant
L	gap length
m	mass
p'	pressure gradient of the Bingham fluid
p'_n	pressure gradient of the Newtonian fluid
p'_c	the smallest pressure gradient between stationary plates
P	non-dimensional total pressure gradient
Q	volumetric flow rate of Bingham flow
Q_s	volumetric flow rate of pure-shear
r	piston head radius
T	non-dimensional pressure gradient due to yield shear stress
U	relative velocity of two plates
v_p	piston velocity
V	non-dimensional velocity
w	gap width
x_b	displacement of the base
x_m	displacement of the mass
ϕ_c	Bingham number
ϕ_D	dynamic range
ϕ_F	non-dimensional damping force
ϕ_r	non-dimensional geometric parameter
η	zero-field viscosity of the Bingham fluid
τ_y	yield shear stress of the Bingham fluid

This change is primarily observed as a significant increase of the yield shear stress of the fluids and can be continuously controlled by tuning the intensity of the applied field. Thus, ER or MR fluids can be effectively utilized in vibration control of various dynamic systems including vehicle shock absorbers, dampers, and mounts [1–4].

It is advantageous to develop a non-dimensional model that can predict the field-dependent pressure drop or damping force in an ER or MR damper in order to determine appropriate design parameters for favorable vibration control performance. So far, several non-dimensional models have been developed by considering operational modes of ER or MR fluids, and used to analyze pressure drop or damping force of ER or MR valves and/or dampers. Phillips [5] cast the Bingham plastic flow equations for Poisieulle flow through a rectangular duct as a set of non-dimensional groups and corresponding polynomial equations that determine the pressure gradient of ER fluid under Poisieulle flow (flow mode), as well as mixed Poisieulle and Couette flow (mixed mode) operations. Makris et al. [6] described a dimensional equation can be efficiently used to predict the damping force of an ER damper with an annular bypass. Gavin et al. [7] and Gavin [8] presented an approximation to the exact solution of a non-dimensional polynomial which has a complex form, and showed that this approximation is useful in designing ER devices operating under flow or mixed mode operation. Stanway et al. [1], Peel et al. [9] and Williams et al. [10] developed a non-dimensional form that reduces the number of design parameters required to predict pressure drop of the ER or MR device operated under flow or squeeze mode. Wereley and Pang [11] and Lindler and Wereley [12] presented a set of non-dimensional groups characterizing equivalent viscous damping constant of ER and MR dampers. This non-dimensionalization scheme is very useful for the analysis of ER and MR damper operating under flow or mixed mode operation. Recently,

Hong et al. [13] developed a non-dimensional analysis and design scheme for a flow mode ER damper. This non-dimensional analysis is effective in predicting the field-dependent damping force and dynamic range. Furthermore, the design specifications for the flow mode ER damper can be efficiently set by considering the vibration control performance of an application system.

In the present work, a non-dimensional analysis scheme and non-dimensional design methodology for an MR damper under mixed mode operation are developed. The non-dimensional analysis model of the MR damper utilizes four non-dimensional parameters: Bingham number, non-dimensional damping force, dynamic range, and non-dimensional geometric parameter defined as the ratio of the piston (or plunger) radius to the annular gap size. The non-dimensional scheme is analytically verified and the influence of the non-dimensional parameters is also investigated. The proposed non-dimensional design scheme is assessed via an MR isolation mount case study. The MR mount consists of a rubber element and an MR damper. Design specifications of the maximum damping force and the dynamic field-controllable force range are set by considering the sky-hook control performance of a single dof system. The principal design parameters of the MR damper, to be incorporated into the system, are determined on the basis of a non-dimensional design procedure. Finally, the MR damper is manufactured and its field-dependent damping forces are experimentally evaluated to validate the effectiveness of the proposed non-dimensional analysis and design methodology.

2. Non-dimensional analysis of MR damper

The schematic configuration of the proposed MR damper, operating in mixed mode, is shown in Fig. 1(a). The MR damper consists of an MR fluid, plunger (or piston), annular gap, electromagnet coil, flux guide, and housing. The MR fluid fills the annular gap between the plunger and outer cylindrical housing. The cross-sectional area of the plunger is the effective piston area. The electromagnet coil in the housing provides the magnetic field in the annular gap. During relative motion between the plunger and housing, MR fluid flows through the annular gap. Thus, the pressure drop due to flow resistance of MR fluid in the annular gap is induced. At the same time, the MR damper has additional shear resistance due to relative motion between the annular gap walls. Therefore, the proposed MR mount operates under both flow and shear modes. If no magnetic field is applied, the MR damper produces a damping force caused only by the fluid resistance associated with the viscosity of the MR fluid. However, if a certain level of magnetic field is applied through the annular gap, the MR damper produces a controllable damping force due to the yield stress of the MR fluid.

A set of non-dimensional parameters and a corresponding quintic polynomial [5] to determine the pressure gradient of the mixed mode flow of Bingham fluid in a rectangular gap is

$$P^3 - (1+3T)P^2 + 4T^3 + P^2V + \frac{P^2TV^2}{3(P-2T)^2} = 0, \tag{1}$$

where

$$P = \frac{p'}{p'_n}, \quad T = \frac{p'_c}{2p'_n}, \quad V = \frac{Q_s}{Q}. \tag{2}$$

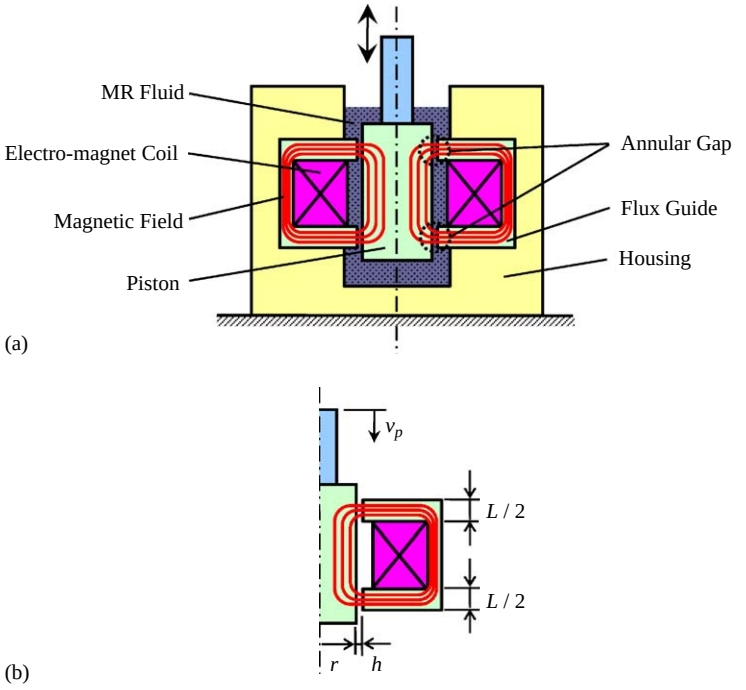

Fig. 1. The proposed MR mixed-mode damper; (a) configuration, (b) geometry.

In the above, the non-dimensional pressure gradient, P, is the ratio of the pressure gradient of Bingham fluid, p', to the pressure gradient of Newtonian fluid, p'_n. In other words, the non-dimensional parameter, P, represents the dynamic range, which is the ratio of the field-induced pressure gradient to the zero-field pressure gradient at the same flow rate. The non-dimensional yield shear stress, T, is the ratio of the smallest pressure gradient, p'_c, that can exist when flow occurs between two plates to the pressure gradient of Newtonian fluid, p'_n. Non-dimensional velocity, V, is the ratio of the volumetric flow rate of pure-shear, Q_s, to the volumetric flow rate of Bingham flow, Q. When the non-dimensional velocity, V, approaches zero, Eq. (1) represents solely flow mode operation of the damper.

On the other hand, the dimensional parameters of Eq. (2) are given by

$$p'_n = \frac{12Q\eta}{wh^3}, \quad p'_c = \frac{2\tau_y}{h}, \quad Q_s = \frac{whU}{2}. \tag{3}$$

In the above, τ_y and η are the field-dependent yield shear stress and post-yield plastic viscosity of Bingham fluid, respectively. Also, w is the gap width, h is the gap size and U is the relative velocity between the annular gap walls. If the ratio of the piston radius to the gap size is large, Eqs. (1)–(2), which represent the mixed mode flow of a Bingham fluid in a rectangular gap, can be applied to approximate the mixed mode flow through the annular gap [7]. Furthermore, the physically meaningful root of the non-dimensional equation (1) can be represented by the following

simplified form:

$$P = a + bT - cV. \tag{4}$$

In order to minimize approximation error, a, b and c must be selected by considering an appropriate range of non-dimensional pressure gradient as a function of the field-dependent yield stress T. When, the parameter c is zero, Eq. (4) reduces to the result for the flow mode of operation for a Bingham fluid. Furthermore, when the parameter b is zero, Eq. (4) represents Newtonian flow in the absence of Bingham effect or zero yield stress. The parameters a, b, and c for the mixed mode operation of a Bingham fluid have been chosen such that approximation error to the exact solution of quintic polynomial (1) over the specific range of T is minimized. The approximation result is shown in Fig. 2, and the parameters were chosen in this study to be $a = 1$, $b = 2.47$ and $c = 1$. It is observed that the approximate solution (4) shows favorable accuracy in the considered range of T. Thus, Eq. (4) is used for the non-dimensional analysis undertaken in this work.

From the MR damper geometry shown in Fig. 1(b), the volume flux, Q, and valve width, w, of the MR damper can be expressed as

$$Q = A_p U = -A_p v_p, \quad A_p = \pi r^2, \tag{5}$$

$$w = 2\pi(r + h/2) \approx 2\pi r. \tag{6}$$

In the above, A_p is the piston head area (or cross-sectional area of the piston), r is the piston radius and $v_p(= -U)$ is the piston velocity. By substituting Eqs. (2), (3), (5), (6) into Eq. (4), the dynamic ratio, ϕ_D, defined by the ratio of the total damping force, F_{mr}, to the viscous damping force, F_v, can be expressed as

$$\phi_D = \frac{F_{\mathrm{mr}}}{F_v} = \frac{a + bT - cV}{a - cV} = 1 + \frac{b}{6}\frac{\phi_c}{a\phi_r + c}, \tag{7}$$

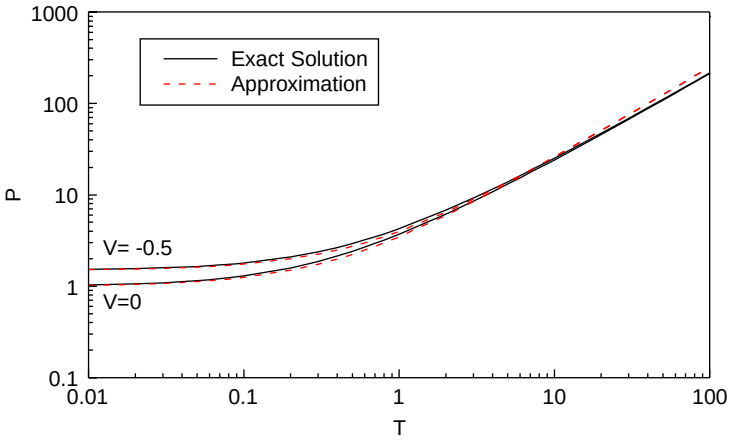

Fig. 2. Approximation of exact solution of the non-dimensional equation.

where

$$\phi_c = \frac{\tau_y h}{\eta v_p}, \quad \phi_r = \frac{r}{h}. \tag{8}$$

In the above, the non-dimensional parameter ϕ_c is the well-known Bingham number and represents the ratio of the dynamic yield shear stress to the viscous shear stress [11,14]. In addition, ϕ_c shows the influence of the magnetic field on the damping force of the MR damper. The non-dimensional parameter ϕ_r represents the geometric ratio characterized by the piston radius r and gap h. The geometric ratio is proportional to the hydraulic amplification or the ratio of the piston area to the annular gap area, $\phi_r \propto A_p/wh$. On the other hand, the damping force (F_{mr}) of the MR damper is given by

$$F_{\mathrm{mr}} = p' L A_p, \tag{9}$$

where L is the length of the effective region of the annular gap. Now, substituting Eqs. (2)–(6), (8) into Eq. (9) yields the non-dimensional damping force, ϕ_F, represented by the non-dimensional parameters ϕ_c and ϕ_r as follows:

$$\phi_F = a\phi_r^3 + \left(\frac{b}{6}\,\phi_c + c\right)\phi_r^2. \tag{10}$$

Thus, the damping force of the MR damper can be expressed by

$$F_{\mathrm{mr}} = (6\pi\eta v_p L)\phi_F. \tag{11}$$

It is observed from Eq. (11) that the damping force F_{mr} can be directly scaled by the gap length L. When the Bingham number ϕ_c is zero, Eq. (10) reduces the equation of the damping force for the case of Newtonian flow.

The relationship between the dynamic ratio ϕ_D and the non-dimensional geometric parameter ϕ_r is illustrated in Fig. 3(a) as the Bingham number ϕ_c is varied. As the Bingham number ϕ_c increases, the dynamic range ϕ_D of the MR damper also increases. The Bingham number ϕ_c is large when the piston velocity v_p is low, or the yield shear stress τ_y is high. Thus, a large value of ϕ_c implies that the MR damper operates close to the yield stress of the MR fluid. For a given Bingham number, as the non-dimensional geometric parameter ϕ_r increases, the dynamic ratio ϕ_D decreases. Thus, small piston radius r or large gap size h are preferred to maximize dynamic ratio ϕ_D. Furthermore, the gap size h has a great influence on both non-dimensional parameters ϕ_c and ϕ_r. Enlarging the gap size h increases the Bingham number ϕ_c and decreases the non-dimensional geometric parameter ϕ_r. Thus, dynamic range ϕ_D can be maximized by increasing the gap size h, although h is limited due to field considerations.

The relationship between the non-dimensional damping force ϕ_F and the non-dimensional geometric parameter ϕ_r is presented in Fig. 3(b) as the Bingham number, ϕ_c, is varied. The non-dimensional damping force ϕ_F increases as both the Bingham number, ϕ_c, and the non-dimensional geometric parameter, ϕ_r, increase. This implies that high-yield shear stress, τ_y, large piston radius, r, and small gap size, h, are all required to exert high damping force using a damper. On the other hand, large piston radius, r, and small gap size, h, will reduce the dynamic range, ϕ_D, and may deteriorate vibration control performance of the overall MR damper system.

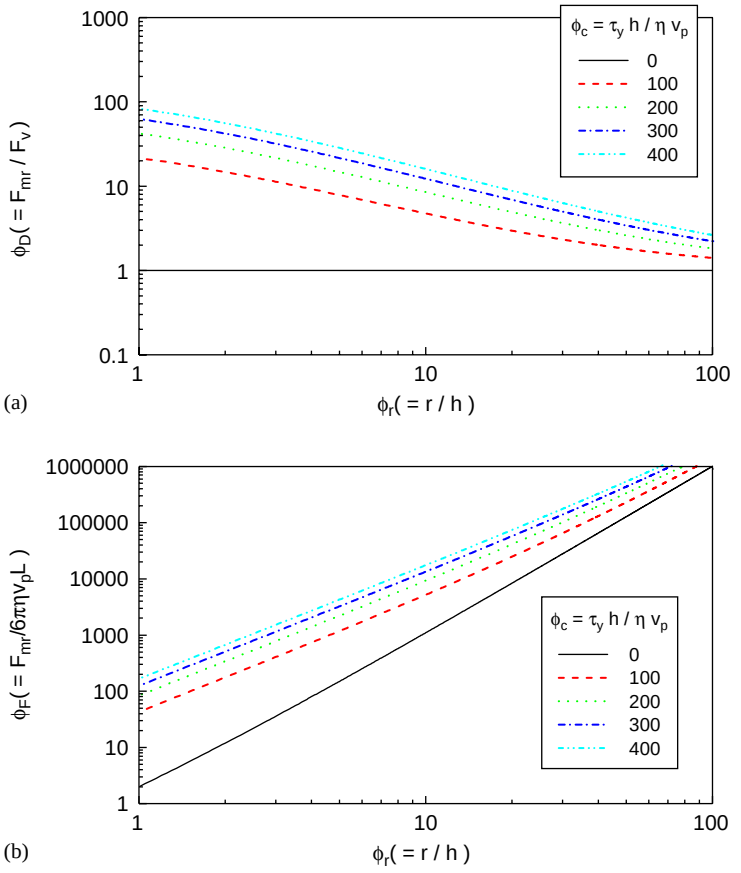

Fig. 3. Analytical verification of the non-dimensional equations; (a) $\phi_D - \phi_r$ relation, (b) $\phi_F - \phi_r$ relation.

3. Design of MR damper

Using the non-dimensional forms and parameters of Eqs. (7), (8), (10), (11), effective design procedures for the MR devices such as dampers and mounts can be established to meet the imposed design requirements. In general, the dynamic range, ϕ_D, and maximum damping force, F_{mr}, are imposed as the most important design requirements in MR dampers. Therefore, in order to meet the desired dynamic range and maximum damping force, the appropriate design procedure of MR damper should be developed. Then, the design steps can be summarized as follows:

(i) Specify the dynamic range $\phi_D(= F_{\mathrm{mr}}/F_v)$: given design requirement or constraint.
(ii) Specify the maximum damping force F_{mr} at the piston velocity v_p: given design requirement or constraint.
(iii) Measure the Bingham-plastic properties of the employed MR fluid (τ_y, η).
(iv) Calculate the Bingham number $\phi_c(= \tau_y h/\eta v_p)$ using Eq. (8) by the substitution of τ_y and η of step (iii), and considering appropriate gap size h.

(v) Find the geometric parameter ϕ_r which meets the desired dynamic range ϕ_D of step (i) using Eq. (7) by the substitution of h of step (iv). In this step, the piston head radius $r(=\phi_r h)$ is achieved.
(vi) Find the non-dimensional force ϕ_F using Eq. (10) by the substitution of ϕ_c^* of step (iv) and ϕ_r of step (v).
(vii) Calculate the electrode length L using Eq. (11) by the substitution of η of step (iii) and F_{mr} at v_p of step (ii).

In order to demonstrate the effectiveness of the proposed design procedure, a MR mount is considered and its schematic configuration is presented in Fig. 4. The MR mount was constructed by incorporating both a rubber element and an MR damper. The passive mount utilizing the rubber elements has been widely adopted to support a static load and to isolate a dynamic load over high and post-resonance frequency range. The top end of the rubber element has fixture with which to support the vibrating mass and is connected to the piston of the MR damper. The bottom plate of the rubber element is attached to the MR damper housing.

First, the maximum damping force F_{mr}, the piston velocity, v_p, and the dynamic ratio, ϕ_D, of steps (i) and (ii) are specified by considering the vibration model shown in Fig. 5. The governing equation of the vibration model is obtained by

$$m\ddot{x}(t) = -k_r(x_m(t) - x_b(t)) - c_r(\dot{x}_m(t) - \dot{x}_b(t)) - c_f(\dot{x}_m(t) - \dot{x}_b(t)) - f_c(t). \tag{12}$$

In the above, m is the mass supported by the MR mount. k_r and c_r are the spring and damping constant of the rubber element, respectively. c_f is the damping exerted by the flow resistance of the MR damper in the absence of magnetic field, and $f_c(t)$ is the damping force which can be controlled by the intensity of the magnetic field. $x_m(t)$ is the displacement of the mass, and $x_b(t)$ is the displacement of the base excitation. The parameters of the mass and rubber element, adopted for this test model, are listed as follows: $m = 12\,\mathrm{kg}$, $c_r = 140\,\mathrm{N\,s/m}$, and $k_r = 106\,\mathrm{kN/m}$.

Prior to determining the design parameters, uncontrolled responses were analyzed. The amplitude of the sinusoidal excitation velocity $\dot{x}_b$ was set to be 0.01 m/s. The mass velocity $\dot{x}_b$ and the piston velocity $v_p(=\dot{x}_m - \dot{x}_b)$ are presented in Fig. 6(a) and (b). The maximum mass velocity is limited to the 0.07 m/s by setting the viscous damping constant c_f of 20 N s/m. Fig. 6(c) shows the

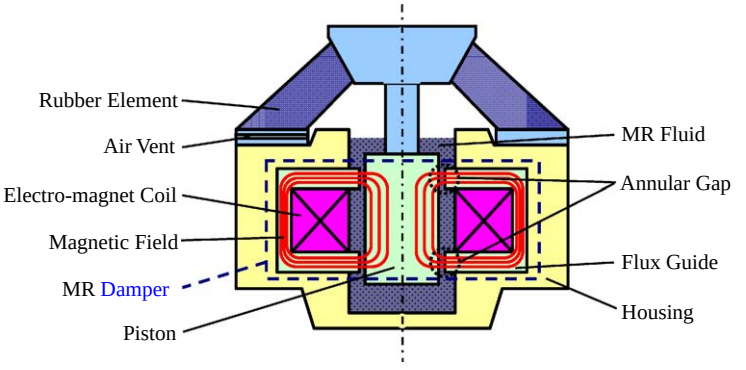

Fig. 4. Schematic configuration of the MR mount.

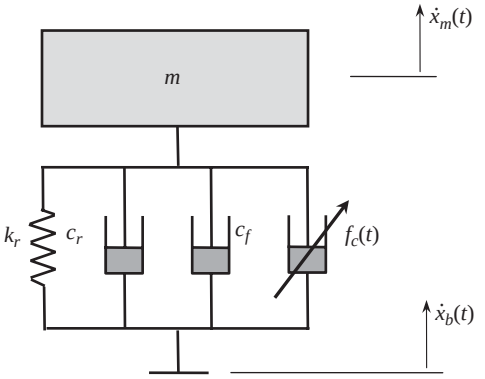

Fig. 5. Vibration model with the MR mount.

viscous damping force obtained from the product of the damping constant and piston velocity. The maximum viscous damping force corresponding to the maximum piston velocity of 0.07 m/s was 1.54 N. As a next step, vibration control performance of the MR mount system was investigated. The sky-hook controller [15], which is a simple and effective control algorithm for the vibration attenuation, was adopted in this work. The control input which directly represents controllable damping force is given by

$$f_c(t) = c_{\text{sky}}\dot{x}_m(t), \tag{13}$$

where c_{sky} is the constant gain for the sky-hook controller. This gain physically implies damping. The damping force should be applied according to the semi-active condition as follows [15]:

$$f_c(t) = \begin{cases} f_c(t) & \text{for } \dot{x}_m(\dot{x}_m - \dot{x}_b) > 0, \\ 0 & \text{for } \dot{x}_m(\dot{x}_m - \dot{x}_b) \leqslant 0. \end{cases} \tag{14}$$

This condition indicates that the actuating of the controller $f_c(t)$ only assures the increment of energy dissipation of the stable system. Fig. 7(a) compares the mass velocity between the controlled and uncontrolled cases. It is observed that the velocity near the resonant frequency is effectively attenuated by activating the MR mount. The control input magnitude is presented in Fig. 7(b), and the maximum value of the control force was 10.7 N. The design specifications of steps (i, ii); dynamic ratio ϕ_D, maximum damping force F_{mr}, and piston velocity v_p, were determined by investigating control performance of the MR mount system. In this work, the maximum damping force was chosen to be $F_{\text{mr}} = 15.4$ N by considering a safety factor and the dynamic ratio was chosen to be $\phi_D = 10$. These values were used for the design of the MR damper.

The field-dependent yield shear stress of the MR fluid (MRF-132LD, Lord Corporation) was experimentally determined to be $\tau_y(H) = 0.13H^{1.13}$ kPa. Here, the unit of magnetic field H is kA/m. The post-yield plastic viscosity was also experimentally evaluated to be $\eta = 0.59$ Pa s. The upper limit of the yield stress of the MR fluid was 4 kPa for a magnetic field of $H = 20.7$ kA/m. From step (iv), the Bingham number at $H = 20.7$ kA/m is $\phi_c = 145.3$. It is noted that the gap size

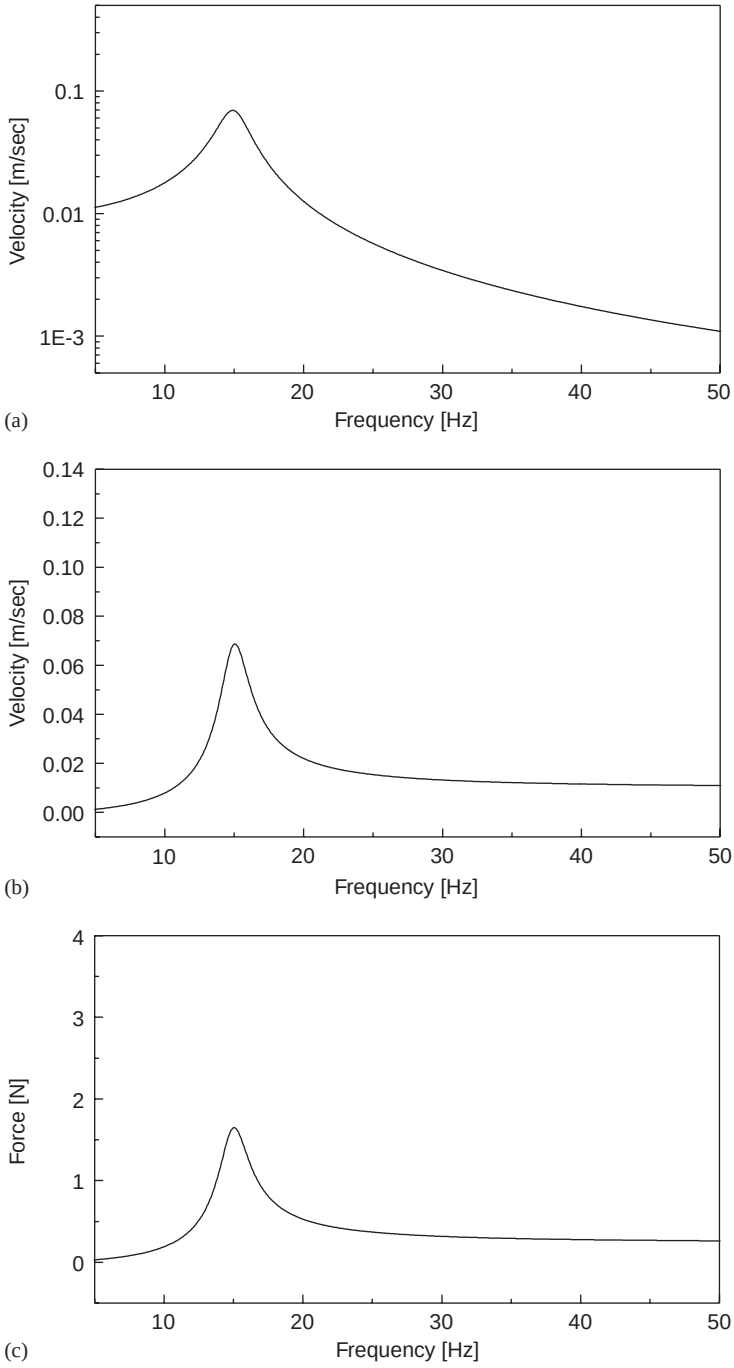

Fig. 6. Uncontrolled responses of the MR mount system; (a) mass velocity $\dot{x}_m$, (b) piston velocity v_p, (c) viscous damping force F_v.

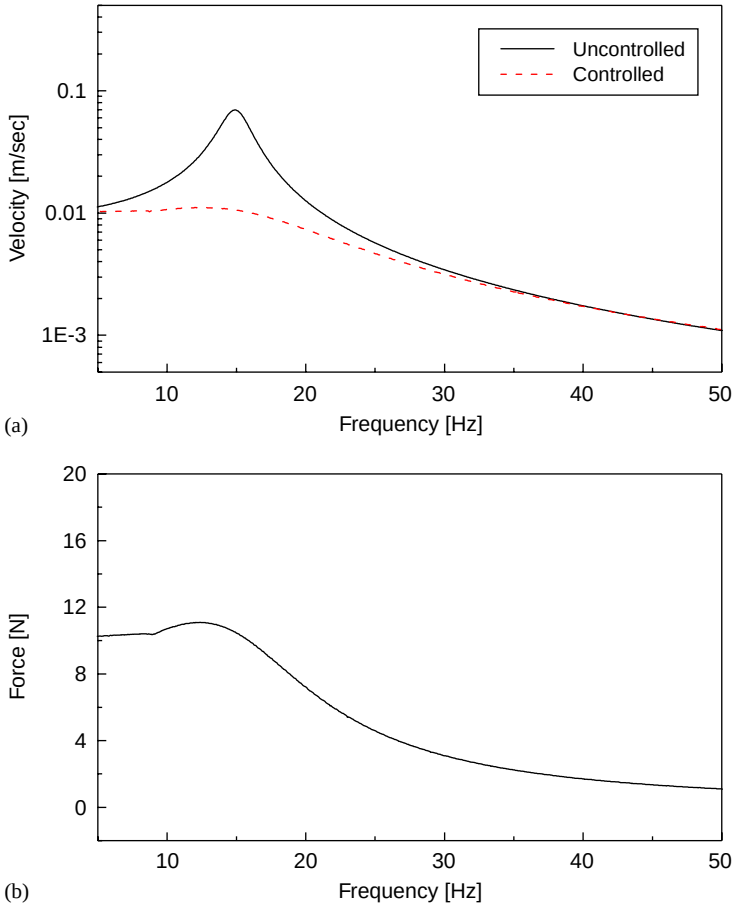

Fig. 7. Controlled responses of the MR mount system; (a) mass velocity $\dot{x}_m$, (b) control force f_c.

has been chosen to be $h = 1.5$ mm by past experience. Fig. 8(a) shows the dynamic range with respect to the geometric parameter at the Bingham number, $\phi_c = 145.3$. To meet the desired dynamic ratio $\phi_D = 10$, the geometric parameter was required to be $\phi_r = 5.6$. Then, the piston head radius was set to be $r = 8.5$ mm according to step (v). Fig. 8(b) presents the relationship between the non-dimensional damping force ϕ_F and the geometric parameter ϕ_r for a Bingham number $\phi_c = 145.3$. The non-dimensional force at the non-dimensional geometric parameter $\phi_r = 5.6$ was found to be $\phi_F = 2134$. Finally, the gap length was determined to be $L = 10$ mm according to steps (vi, vii).

4. Design assessment

Based on the design parameters (L, r, h) determined by the above non-dimensional design scheme, a mixed mode-type MR damper, pictured in Fig. 9, was manufactured. To measure the

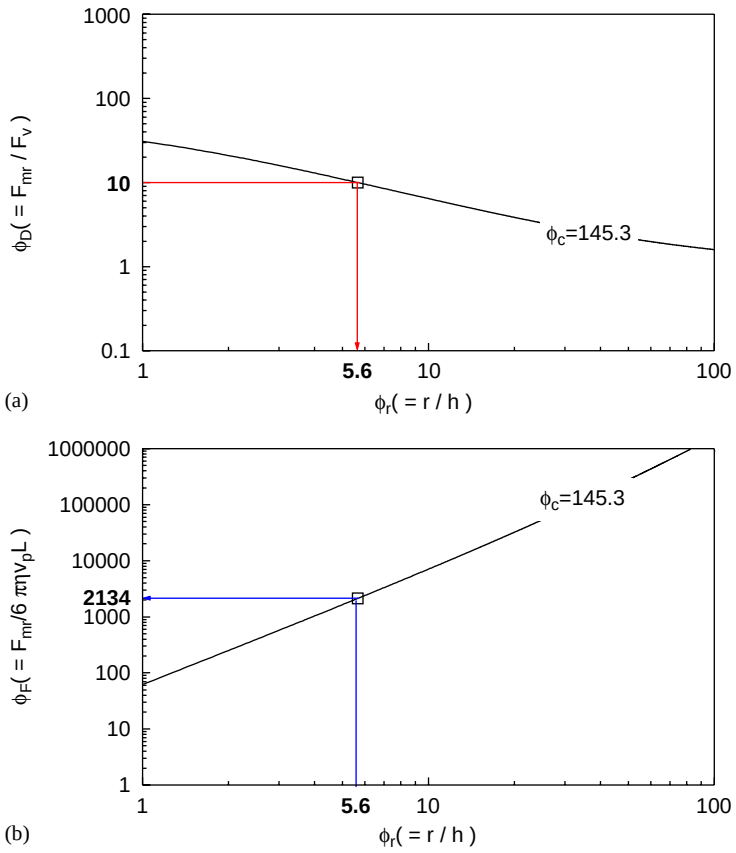

Fig. 8. Non-dimensional design of the MR damper; (a) ϕ_D and ϕ_r at $\phi_c = 145.3$, (b) ϕ_F and ϕ_r at $\phi_c = 145.3$.

field-dependent damping force of the MR damper, the experimental setup presented in Fig. 10 was used. The MR damper is placed between the load cell and an electromagnetic shaker. The accelerometer measures the acceleration of the shaker table, and the signal generated from this accelerometer is fed back to the controller that regulates excitation velocity. When the shaker table moves up and down by a command signal generated from the shaker controller, the MR damper produces a damping force that is measured by the load cell. The excitation velocity signal is measured by using an accelerometer and the charge amplifier which has an integrator. The force and velocity signals are saved in a micro-processor via an A/D (analog to digital) converter. The current is applied to the MR damper via a D/A (digital to analog) converter and a current amplifier. The sinusoidal excitation velocity amplitude and frequency were selected as 0.07 m/s and 15 Hz, respectively.

Fig. 11 compares the predicted and measured values of the dynamic range ϕ_D and non-dimensional damping force ϕ_F of the MR damper designed and manufactured in this study. The effect of the magnetic field intensity is also presented in Fig. 10. It is observed that the measured and predicted values correlate well demonstrating the effectiveness of the proposed non-dimensional scheme. Fig. 12(a) shows the time responses of predicted and measured damping

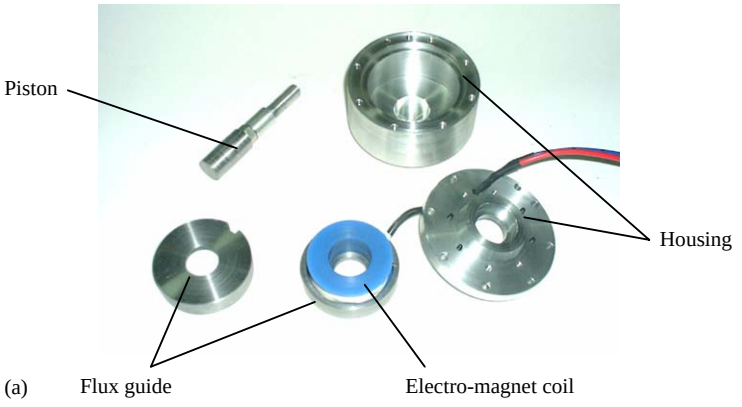

Fig. 9. Photograph of the MR damper; (a) components, (b) assembly.

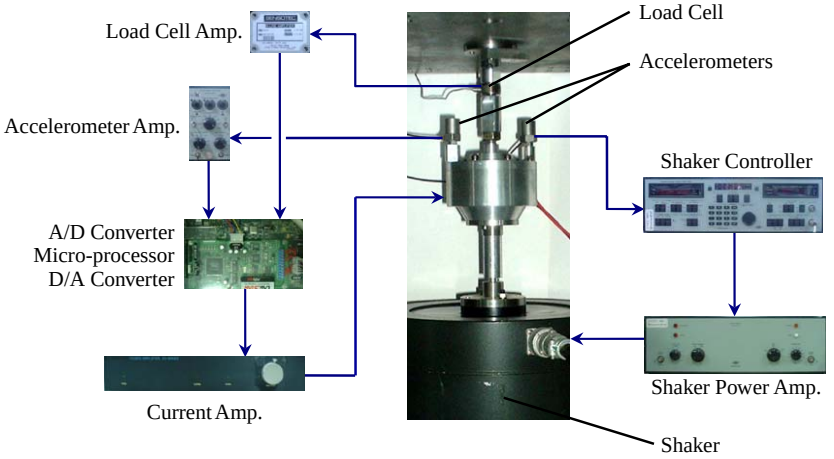

Fig. 10. Configuration of experimental setup.

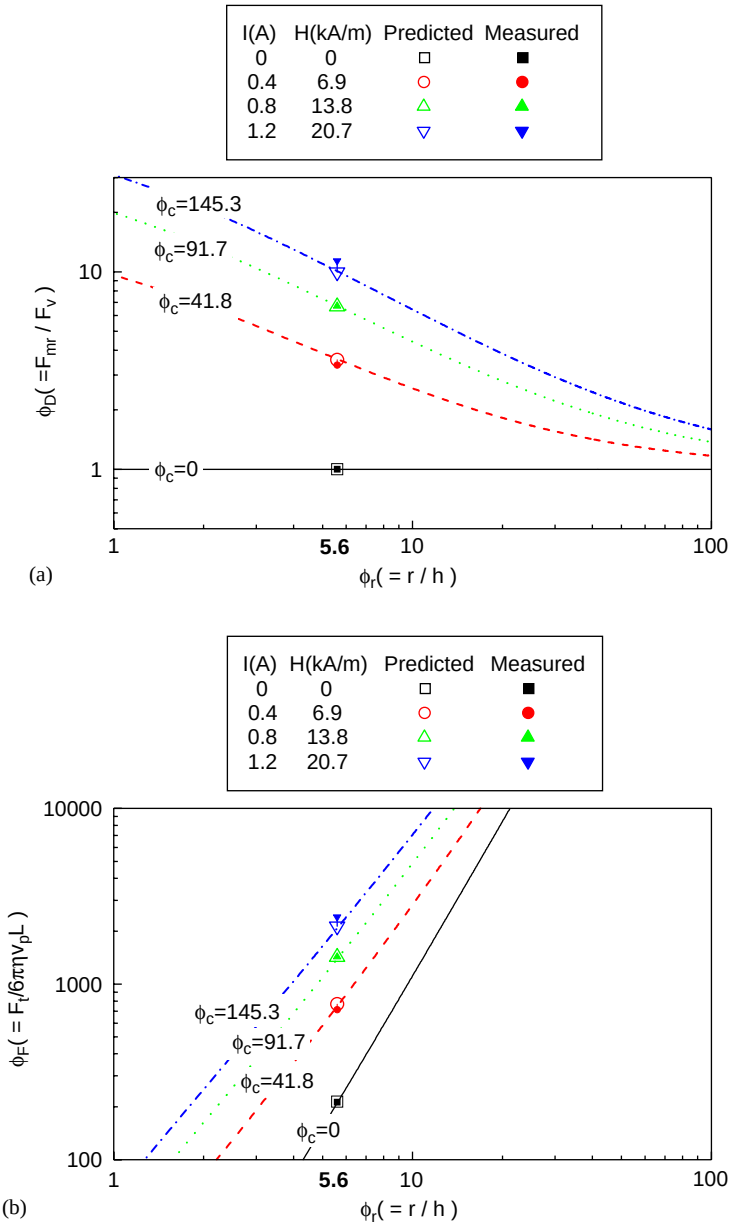

Fig. 11. Comparison of the non-dimensional parameters between the prediction and measurement; (a) predicted and measured ϕ_D, (b) predicted and measured ϕ_F.

forces under various magnetic-field intensities. The damping force versus piston velocity is also presented in Fig. 12(b). The predicted damping forces were obtained by Eq. (10). It is observed that the predicted field-dependent damping force agrees well with the measured force in the post-yield velocity regions. Field-dependent damping force characteristics under various excitation

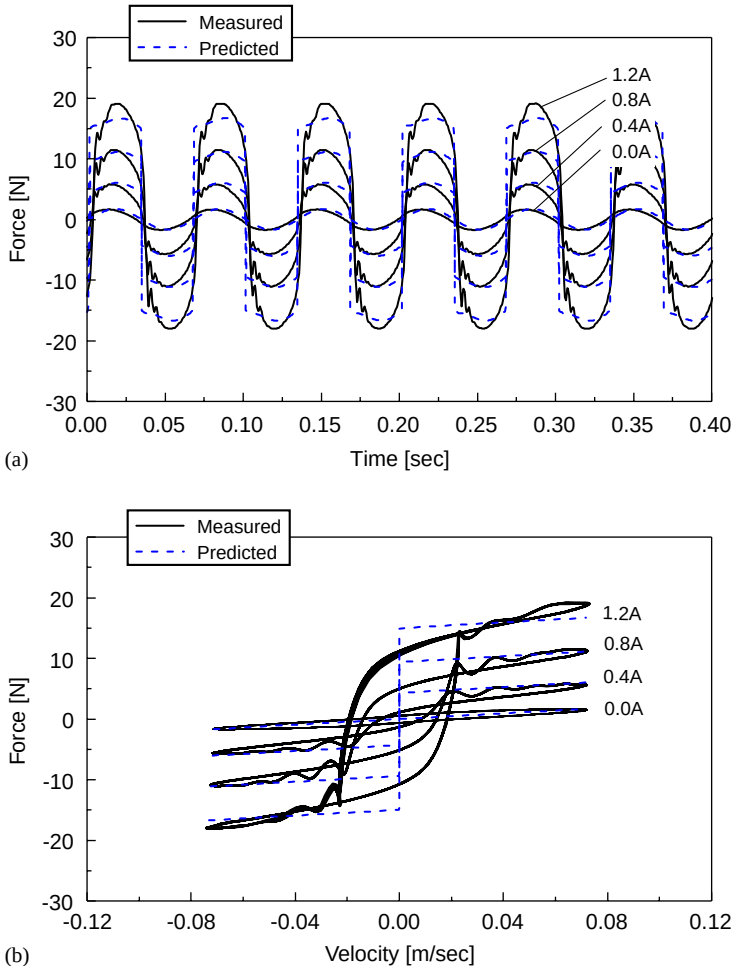

Fig. 12. Comparison of the field-dependent damping forces between the prediction and measurement; (a) damping force vs. time, (b) damping force vs. piston velocity.

frequencies and amplitudes are presented in Fig. 13. The measured damping forces at higher excitation frequencies to Fig. 12 are shown in Fig. 13(a) and (b). As the excitation frequency increases, the slope of low-velocity hysteresis loop decreases and magnitude of inertia loop at velocity extremities increases. The dynamic behaviors of damping force are mainly due to the compliance and fluid inertia effects. On the other hand, Fig. 13(c) and (d) shows the damping force behaviors at lower excitation velocity amplitudes to Fig. 13(a). It is also observed that the low-velocity hysteresis loop and high-velocity inertia loop depend on the excitation velocity amplitudes. But the overall behavior of the damping forces under various excitation conditions in Fig. 13 agrees well with the predictions obtained by using the proposed model in this study. Thus, the effectiveness of the non-dimensional design procedure for the MR damper operated under the mixed mode operation has been proved. Most of previous studies on non-dimensionalization of ER or MR devices have been limited to analysis of damping force characteristics only. By using

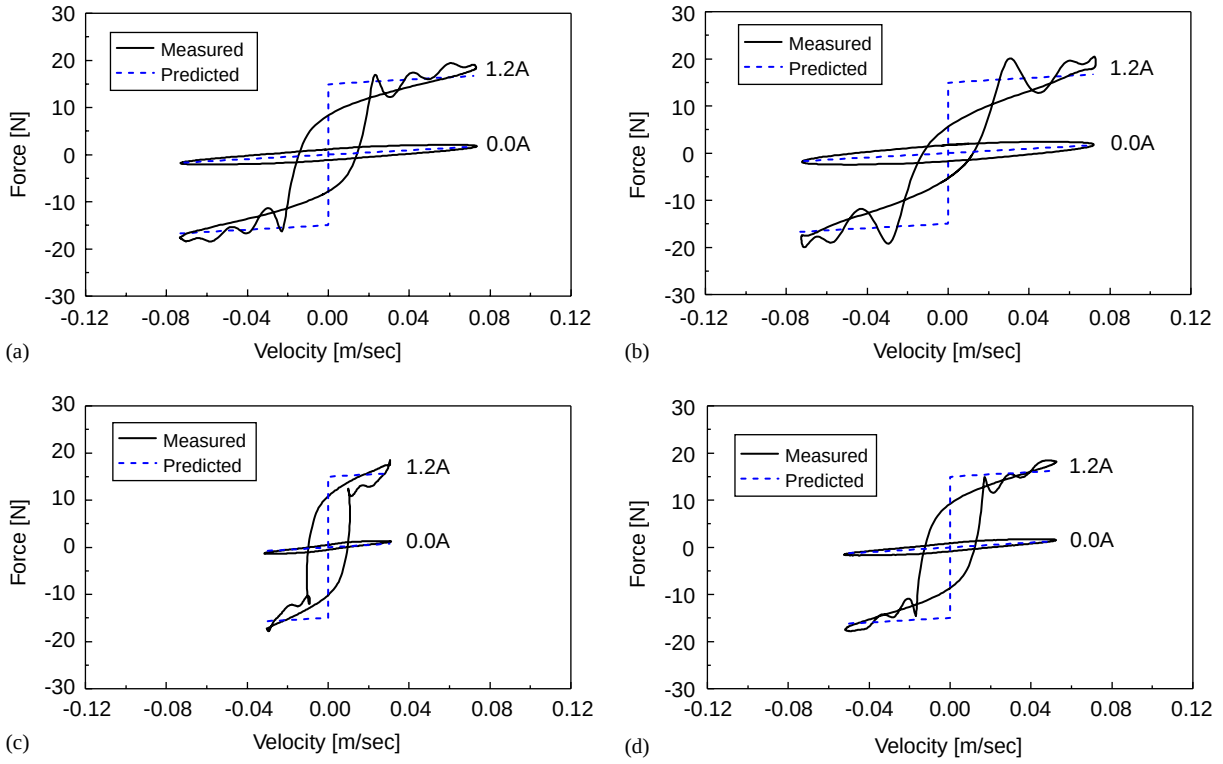

Fig. 13. Field-dependent damping forces under various excitation conditions; (a) excitation: 0.07 m/s, 20 Hz, (b) excitation: 0.07 m/s, 30 Hz, (c) excitation: 0.03 m/s, 20 Hz and (d) excitation: 0.05 m/s, 20 Hz.

the proposed non-dimensional form, both damping force level and dynamic range of the vibration control system can be effectively analyzed.

5. Conclusion

In this study, a non-dimensional design scheme for a MR mixed-mode damper was developed. On the basis of the Bingham plastic constitutive equation of the MR fluid, four non-dimensional design parameters were defined: Bingham number, damping force, dynamic range and geometric ratio (or hydraulic amplification). After investigating design characteristics of each parameter, sequential design steps for the MR damper were formulated and a single dof vibration model consisting of the spring and the MR damper was then established in order to demonstrate the effectiveness of the proposed design methodology. By comparing measured and predicted responses, it was demonstrated that the principal design parameters of MR devices, such as length, width and depth of the MR valve, can be easily and effectively determined from the non-dimensional analysis by specifying a set of physical design requirements, such as the maximum damping force. It is finally remarked that the proposed design methodology can be applied to the

design of various types of ER or MR fluid-based vibration isolators such as shock absorbers and mounts without any modification.

Acknowledgements

This work was partially supported by the National Research Laboratory (NRL) program directed by the Korea Ministry of Science and Technology. This financial support is gratefully acknowledged.

References

[1] R. Stanway, J.L. Sproston, A.K. EI-Wahed, Application of electro-rheological fluids in vibration control: a survey, *Smart Materials and Structures* 5 (4) (1996) 464–482.
[2] S.B. Choi, Y.T. Choi, D.W. Park, A sliding mode control of a full-car electrorheological suspension system via hardware in-the-loop simulation, *Journal of Dynamic Systems, Measurement, and Control* 112 (2000) 114–121.
[3] S.B. Choi, H.S. Lee, Y.P. Park, H-infinity control performance of a full-vehicle suspension featuring magnetorheological dampers, *Vehicle System Dynamics* 38 (5) (2002) 341–360.
[4] S.R. Hong, S.B. Choi, M.S. Han, Vibration control of a frame structure using electrorheological fluid mounts, *International Journal of Mechanical Sciences* 44 (10) (2002) 2027–2045.
[5] R.W. Phillips, Engineering Application of Fluids with Variable Yield Stress, DEng Thesis, Department of Mechanical Engineering, University of California, Berkeley, USA, 1969.
[6] N. Makris, S.A. Burton, D.P. Taylor, Electrorheological damper with annular ducts for seismic protection applications, *Smart Materials and Structures* 5 (1996) 551–564.
[7] H.P. Gavin, R.D. Hanson, F.E. Filisko, Electrorheological dampers, part I: analysis and design, *Journal of Applied Mechanics* 63 (1996) 669–675.
[8] H.P. Gavin, Design method for high-force electrorheological dampers, *Smart Materials and Structures* 7 (1996) 664–673.
[9] D.J. Peel, R. Stanway, W.A. Bullough, Dynamic modelling of an ER vibration damper for vehicle suspension applications, *Smart Materials and Structures* 5 (1996) 591–606.
[10] E.W. Williams, S.G. Rigby, J.L. Sproston, R. Stanway, Electrorheological fluids applied to an automotive engine mount, *Journal of Non-Newtonian Fluid Mechanics* 47 (1993) 221–238.
[11] N.M. Wereley, L. Pang, Non-dimensional analysis of semi-active electrorheological and magnetorheological dampers using approximate parallel plate models, *Smart Materials and Structures* 7 (1998) 732–743.
[12] J. Lindler, N.M. Wereley, Analysis and testing of electrorheological bypass dampers, *Journal of Intelligent Material Systems and Structures* 10 (1999) 363–376.
[13] S.R. Hong, S.B. Choi, Y.T. Choi, N.M. Wereley, Non-dimensional analysis for effective design of semi-active ER damping control systems, *Proceedings of the Institution of Mechanical Engineers, Part D: Journal of Automobile Engineering* 217 (D12) (2003) 1095–1106.
[14] W. Prager, *Introduction to Mechanics of Continua*, Ginn and Company, New York, 1961.
[15] D. Karnopp, Design principles for vibration control systems using semi-active dampers, *Journal of Dynamic Systems, Measurement, and Control* 112 (1990) 449–453.